Theoretical characterization and band gap tuning of $Sn_x(GeSe_2)_{100-x}$ thin films

Dr. Sudhir Kumar Mishra,

Principal,
S.S. College, Jehanabad,

***Abstract*: The ternary compounds $Sn_x(GeSe_2)_{100-x}$ ($0 \leq x \leq 24$ at. %) were prepared in glassy thin films. Using the chemical bond approach, theoretical calculations of effects of Sn content on mean coordination number (CN), constraints number (N_s), molar volume (V_m), compactness (δ), heat of atomization (H_s), cohesive energy (CE), overall difference of electronegativity (Δ_χ) as well as the degree of iconicity (Ion) were discussed. Optical absorbance has been measured in order to evaluate experimentally the band gap (E_g) and the band tail's width (E_e). In addition, conduction-valence bands positions were estimated when changing Sn content. Increasing Sn content from 0 to 24 at. %, decreases E_g from 2.01 to 1.28 eV. Three theoretical estimations of the variations of the band gap with Sn content were critically compared to experimental values. Obviously, the combination of the estimated band gap from Δ_χ and contributions of the formed bonds gives the best adjustment.**

Keywords: Co-ordination Number, Conduction Valance Band, Constraints Number, Heat of Atomization, X-ray diffraction.

Introduction

Glassy chalcogenides belong to a special group of semiconductors that contain one or more chalcogenide elements (S, Se and Te) that belong to VI group of the periodic table. These semiconducting glasses are substantially used in electronics, optics, infrared lenses, optoelectronic, ionic sensors, and ultrafast optical sensors. Selenium based glasses have many technological applications due to their interesting optical properties[1,2]. They have extensive studies because of their uses as photoreceptors in TV Videocon pick-up tubes[3], xerographic machines as well as digital X-ray imaging[4]. Particularly, selenium based binary alloys as Se-Te [5], Se-Ge[6], Se-Sn[7], Se-Sb[8], Se-ln [9] and Se-Zn were the focus of many researchers. These forms are extremely important due to their significant characteristics such as large hardness, high sensitivity and electrical conductivity as well as smaller aging effects in comparison with pure a-Se. The addition of a third dopant not only enlarges the glass formation region, but also improves the physical properties. Thus, the present study is focusing on the ternary Ge-Se-Sn glassy system. These glasses were extensively studied, particularly their electrical[10], thermoelectric[11], optical [12], photoconductivity [13], structure [14], and crystallization kinetics [15, 16]. Furthermore, Ge-Se-Sn chalcogenides are known by their large glass forming area as well as their wonderful linear and nonlinear optical properties[17,18]. The wide glass forming region makes these chalcogenides excellent candidates for tuning their optical properties by composition changing [19,20].

In the present work, since the hardness and rigidity of the ternary compound $Sn_x(GeSe_2)_{100-x}$ are of primary importance[21], I started by estimating CN, N_s, H_s, and CE theoretically using the chemical bond approach[22,23]. Then the band gap (E_g) and Urbach (E_e) energies were determined from experimental optical absorbance. Besides, the overall difference of electronegativity and degree of ionization were deduced. Due to their importance in device conception, one also calculated the conduction and valence bands positions. In order to point out the band gap tuning by composition, I calculated, with three theoretical methods, the variation of the band gap with Sn content. A critical comparison of the different theoretical estimations of the band gap with the experimental measured ones was finally done.

Experimental details

The common melt quenching method was used to prepare different compositions of bulk glassy chalcogenides $Sn_x(GeSe_2)_{100-x}$ where ($0 \leq x \leq 24$ at. %). High purity (5 N) elements from Sigma–Aldrich were introduced into pre-cleaned silica tubes in proper amounts. High precision balance was used for this purpose. The sample's tubes were continuously evacuated down to 5×10^{-6} Torr then sealed off also under vacuum. The ampoules were introduced in a programmable oven, where the rate of heating 20 K/h was used to reach gradually 1225 K. At this final temperature, samples were maintained for 24 h. In order to ensure the ingots homogeneity, the ampoules were shaken during the whole heating period. Finally, a quenching in ice-water of the ampoules was done to get amorphous compounds. The density of the prepared compounds was measured using Archimedes method using toluene as buoyant media as in Ref.[24]

A thermal evaporation coater Edward 306A was used to prepare thin films of $Sn_x(GeSe_2)_{100-x}$ on glass substrates maintained at room temperature. An Edward FTM5 monitor allowed us to control both evaporation rate and film thickness. The deposited films with thickness in the range 600–650 nm were obtained using a constant deposition rate 0.1 nm/s. A uniform thickness of the prepared films could be obtained by rotating the substrates at ≈30 rpm during normal incidence deposition. An experimental confirmation of the compositions for the different prepared samples was obtained by energy dispersive x-ray spectroscopy (EDX). In addition,

x-ray diffraction using Shimadzu XRD 6000 diffractometer confirmed that, the deposited films were completely amorphous. The film absorbance over 0.45–0.85 μm spectral range has been measured using a Jasco-630 double beam spectrometer.

Results and discussion

The mean coordination number (CN) is attained using the bonding manner in the nearest-neighbor district [25], and the various specifications of non-crystalline chalcogenides are identified. Using the CN of Ge, Se, and Sn listed in Table 1, the following equation is used to calculate the values of CN of the $Sn_x(GeSe_2)_{100-x}$ ($0 \leq x \leq 24$ at. %) glasses:

$$CN = CN(Ge).MF_{Gc} + CN(Se).MF_{Sc} + CN(Se).MF_{Sc} \quad (1)$$

Where.

Table 1 Some physical parameters of Ge, Se and Sn used for calculations.

	Ge	Se	Sn
CN	4	2	4
Hs (kcal/g atom)	90.0	49.4	72.0
BE (kcal mol $^{-1}$)	37.60	44.04	46.70
X	2.01	2.55	1.88
E_g (eV)	0.95	1.95	0
ρ (g/cm^3)	5.10	4.28	7.31

MF_{Se} is the mole fraction for Ge,
MF_{Se} is the mole fraction for Se, MF_{Sn} is the mole fraction for Sn.
The obtained CN value allows the researcher to acquire the Ns, i.e. the constraints number. It is used in order to identify glasses' rigidity. For non-crystalline substances, Ns can be represented as [26]:

$$N_S = {}^{CN}/_{2} + (2CN - 3) \quad (2)$$

CN and N_s were estimated, using the above equations, for the $Sn_x(GeSe_2)_{100-x}$ system and listed in Table 2. Moreover, from Table 2 it is evident, that expansion of Sn content causes an increase in the values of CN and N_s. This property of the glasses is attributed to the increased cross-linkage due to the 4-folds coordination of Sn into the system [27], which ultimately results in an increase of the rigidity of the films.

Lone pair electrons (LP) are defined as those pairs of non-bonding electrons that remain in the valence band. Chalcogenide glasses have lone pair electrons, so they are also known as lone pair glassy semiconductors. The formation of amorphous materials results in a strain force which can be removed by the presence of lone pair electrons. The newly formed chemical bonds linked with non-bonding electrons possess the property of flexibility. The glass formation is improved by using a large number of lone pair electrons through reduced strain energy of the system[28]. The difference between valence electrons (VE) and the mean coordination number (CN) identifies the LP value of the $Sn_x(GeSe_2)_{100-x}$ glasses. i.e.

$$LP = VE - CN \quad (3)$$

Table 2 shows the estimated values of the lone pair electrons. The current study shows that, LP decreases from 2.67 to 2.03 with increasing Sn content from 0 to 24 at. % so, the first glass ($GeSe_2$) is considered the best glass former in this series.
Atomization heat (HS) of $Ge_\alpha Se_\beta Sn_\gamma$ is written as follows [24,29]:

$$H_s \frac{\alpha H_s(Ge) + \beta H_s(Se) + \gamma H_s(Sn)}{\alpha + \beta + \gamma} \quad (4)$$

Table 2 shows the computed values of H_s for $Sn_x(GeSe_2)_{100-x}$ ($0 \leq x \leq 24$ at. %) system, calculated using H_s for the constituent components listed in Table 1. It is evident from Table 2 that, increasing the Sn content leads to an increase of Hs. Taking into account that Hs of Sn (72 kcal/mol) is higher than the overall heat of atomization of $GeSe_2$ (62.93 kcal/mol), one could explain why the overall Hs of $Sn_x(GeSe_2)_{100-x}$ increases with Sn content.

Table 2

Compositional dependence of some physical parameters for the $Sn_x(GeSe_2)_{100-x}$ glassy system.

Sn	CN	N_s	ρ	R	CE	H_s	LP
at.%			g/cm^3		eV	Kcal/mol	
0	2.67	3.67	4.98	1	2.85	62.93	2.67
2	2.69	3.73	5.03	0.94	2.88	63.11	2.63
4	2.72	3.80	5.08	0.89	2.94	63.29	2.56
6	2.75	3.87	5.13	0.84	2.97	63.48	2.51
8	2.77	3.93	5.17	0.79	3.01	63.66	2.47
10	2.80	4.00	5.22	0.75	3.06	63.84	2.40

12	2.83	4.07	5.26	0.71	3.09	64.02	2.35
14	2.85	4.13	5.31	0.67	3.13	64.20	2.35
16	2.88	4.20	5.35	0.64	3.18	64.38	2.24
18	2.91	4.27	5.39	0.60	3.22	64.56	2.19
20	2.93	4.33	5.48	0.57	3.25	64.75	2.15
22	2.96	4.40	5.53	0.54	3.30	64.93	2.08
24	2.99	4.47	5.58	0.51	3.34	65.11	2.03

The values of *BE* (A – B), i.e. the hetero-polar bond energy, are acquired through homo-polar bond energies and the electronegativities; χ_A and χ_B (included in Table 1) of the included atoms which can be seen by the following equation [30,31]:

$$BE\ A-B) = BEA-A).BE(B-B)^{1/2} + 30(X_A - X_A)^2 \quad (5)$$

Distribution of chemical bonds within the $Sn_x(GeSe_2)_{100-x}$ glasses obtained via the chemical bond approach [22,23] is presented in Table 3. The examination shows that Se-Sn, Ge-Se, and Ge-Ge bonds have energies 58.82, 49.44 and 37.60 kcal/mol, respectively. The first composition $GeSe_2$ is called a stoichiometric glass (only Ge-Se bonds are existed) where the deviation of stoichiometry (r) equals one. Values of r were estimated as in Refs. [29] and presented in Table 2. Moreover, it is to be noted in the table that as the Sn concentration increases, the Ge-Se bonds are replaced with Se-Sn and Ge-Ge bonds that increase the average bond energy of the system. Adding bond energies evaluates the energy of cohesive (CE) for glasses and can be calculated by the following equation [32]:

$$CE = \sum (C_i\ BE_i/100)$$

Where;

BE_i is the bond energy and C_i is the number of that bond.

Table 2 presents the values of CE for $Sn_x(GeSe_2)_{100-x}$ ($0 \leq x \leq 24$ at. %) glasses and it is evident from the table that CE increases from 2.85 to 3.34 eV with increasing the Sn content from 0 to 24 at.%.

The increment of CN, N_s, H_s and CE are clear indication for increasing the rigidity of the $Sn_x(GeSe_2)_{100-x}$ glasses by increasing the Sn content. This characteristic is observed due to the increase of cross-linking with the addition of the 4-fold coordinated Sn in place of the overall 2.67 -fold coordinated $GeSe_2$.

The glass compactness (δ) was estimated using the formula [33]:

$$\delta = \frac{\sum_i x_i Am_i \rho_i^{-1}}{\sum_i x_i Am_i \rho_i} - 1 \quad (7)$$

where x_i is atomic percent, Ami is the atomic weight, ρ_i is the atomic density of ith element and ρ is the measured glass density. The mean atomic volume (V_m) was estimated by the relationship:

Table 3

Values of X, E_g, E_{CB} and E_{VB} as well as the distribution of chemical bonds for the $Sn_x(GeSe_2)_{100-x}$ thin films.

Sn	X	E_g	E_{CB}	E_{VB}	D_{Se-Sn}	D_{Ge-Se}	D_{Ge-Ge}
at.%	(eV)						
0	5.42	2.01	0.091	- 1.924	0	1	0
2	5.39	1.95	0.085	- 1.865	0.06000	0.9104	0.0296
4	5.36	1.86	0.067	- 1.794	0.1176	0.8235	0.0589
6	5.34	1.77	0.046	- 1.720	0.175	0.7375	0.0876
8	5.31	1.71	0.017	- 1.668	0.2319	0.6522	0.1159
10	5.28	1.64	0.036	- 1.605	0.2857	0.5714	0.1429
12	5.26	1.61	0.047	- 1.563	0.3404	0.4894	0.1702
14	5.23	1.55	0.043	- 1.507	0.3944	0.408	0.1971
16	5.21	1.49	0.040	- 1.452	0.4445	0.3333	0.2222
18	5.18	1.44	0.039	- 1.400	0.4966	0.2552	0.2482
20	5.15	1.39	0.041	- 1.350	0.5479	0.1781	0.2740
22	5.13	1.33	0.034	- 1.292	0.5946	0.1081	0.2973
24	5.10	1.28	0.034	- 10242	0.6443	0.0336	0.3221

$$V_{m=\rho^{-1}\sum_i A_i Am_i} \quad (8)$$

Fig. 1 shows the compositional dependence of the mean atomic volume and compactness of $Sn_x(GeSe_2)_{100-x}$ glasses. Since Sn is denser and more massive than Se and/or Ge atoms, then increasing its amount leads to an increase of the density. However, the increase of the mean atomic weight with Sn content is faster than the increase of the density leading to an increase of V_m in line with relation (8). Consequently δ decreases. The least square fitting of plots by a linear equation gives for molar volume 0.01x + 15.4 whereas –0.01x + 3.07 for compactness with an adjustment factor about 99% for both.

The absorption coefficient (α) was determined using this relationship (α = (2.3A)/t where t is the film thickness and A is the absorbance [34]. In non-crystalline semiconductors, often indirect transitions describes successfully the absorption mechanism [35].

In such case, the term $(\alpha h\upsilon)^{1/2}$ was plotted versus $h\upsilon$ as shown in Fig. 2. The value of the band gap (E_g) for each glass was determined from the intersect where $h\upsilon = 0$. Values of E_g were inserted in Table 3

On the other hand, for the low absorption range, the photon energy dependence of the absorption coefficient (α) obeys the expression ($\alpha = \alpha_0 \exp(h\upsilon/E_e)$ where E_e is the Urbach's energy).[36]. E_e is considered as a significant parameter that defines the properties of amorphous semiconductors which is linked to the structural disorder. In fact, as the disorder increases, the Urbach tail increases and consequently the band gap decreases. Fig. 3 represents the plots of ln(α) versus $h\upsilon$ for films under study. The reciprocal of the slope gives the E_e value. Fig. 4 shows the variations of E_g and E_e values with Sn content for $Sn_x(GeSe_2)_{100-x}$ films. With increasing the Sn content E_g decreases whereas E_e increases which agrees with Mott and Davies model [37]. According to this model, the band gap width changes in opposite manner compared to the Urbach energy. This last tail width is affected by the degree of disorder and defects in non-crystalline systems.

The overall difference of electronegativity (Δ_χ) in formed chemical bonds of a glassy chalcogenide is experimentally estimated by the Dufy's relationship [38]:

$$\Delta_\chi = 0.2688\, E_g \qquad (9)$$

Using the former relation, I could from the experimentally measured band gap energy estimate Δ_χ. Since the majority of the macroscopic properties in the glassy networks is directly linked to the formed bonds, I could estimate the overall degree of ionicity (*Ion*) as done for simple bonds by Pauling [31]

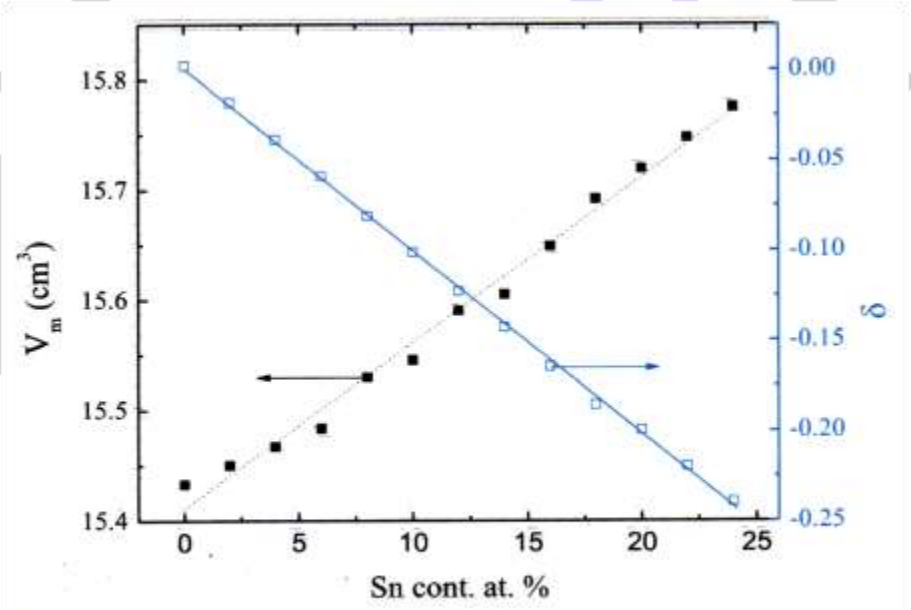

Fig. 1. The compositional dependence of V_m and δ for the $Sn_x(GeSe_2)_{100-x}$ glasses.

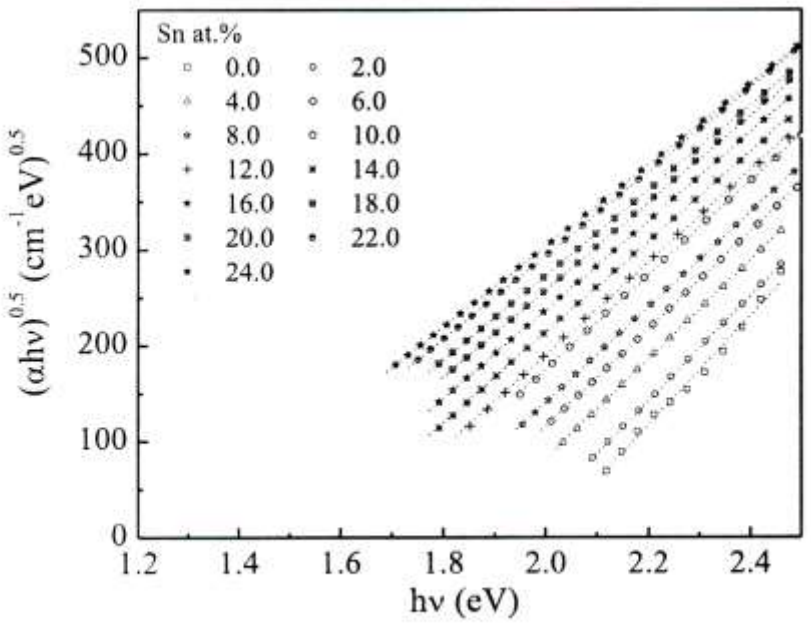

Fig. 2. Variation of $(\alpha h\nu)^{1/2}$ with hν for the $Sn_x(GeSe_2)_{100-x}$ ($0 \leq x \leq 24$ at. %) thin films.

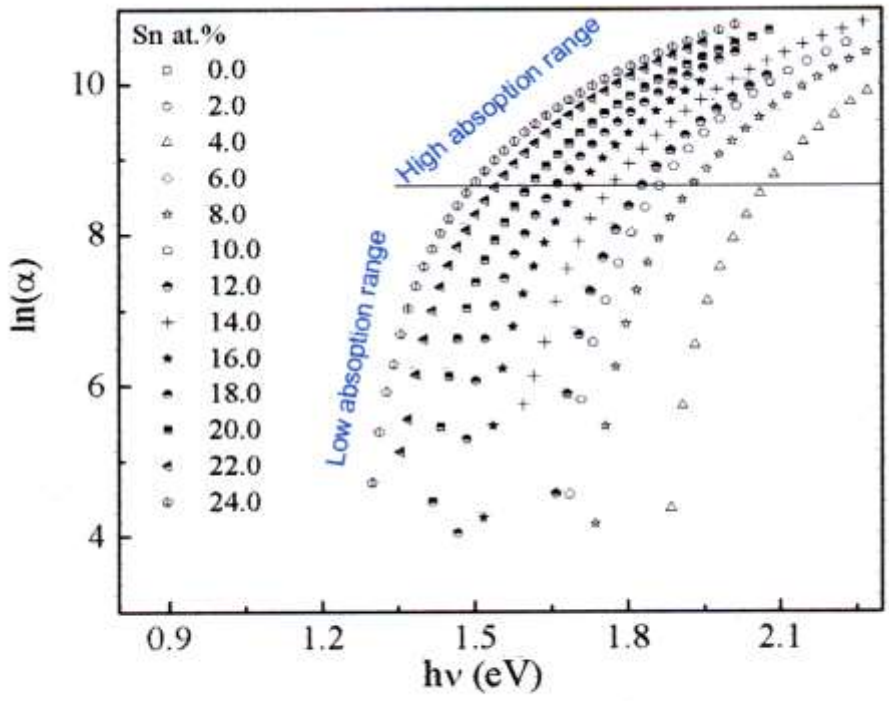

Fig. 3. Plots of ln(α) versus hν for the $Sn_x(GeSe_2)_{100-x}$ ($0 \leq x \leq 24$ at. %) thin films.

$$Ion = 100\left(1 - exp\left[-\frac{\Delta X^2}{4}\right]\right) \quad (10)$$

Fig. 5 shows the obtained values of Δχ and *Ion* versus Sn content. Obviously, since Sn has 4-fold coordination, its introduction increases the compound degree of covalency (*Cov* = 10.exp(– *Δχ*2/4). Consequently, the degree of iconicity decreases as well as Δχ. For composition $Ge_\alpha Se_\beta Sn_\gamma$ the overall band gap energy could be estimated theoretically by three different methods. First, one could write compound band gap as linear combination of element's band gaps (listed in Table 1 [39,40]) taking into account the composition and ignoring element's distribution in space and their bonding:

$$E_g^{(1)} = \alpha.E_g(Ge) + \beta.E_g(Se) + \gamma.E_g(Sn) \quad (11)$$

Obviously, this method cannot give a good approximation to the measured values as depicted in Fig. 6. Second, using the chemical bond approach, one estimates the chemical bond distribution and writes the compound's band gap as:

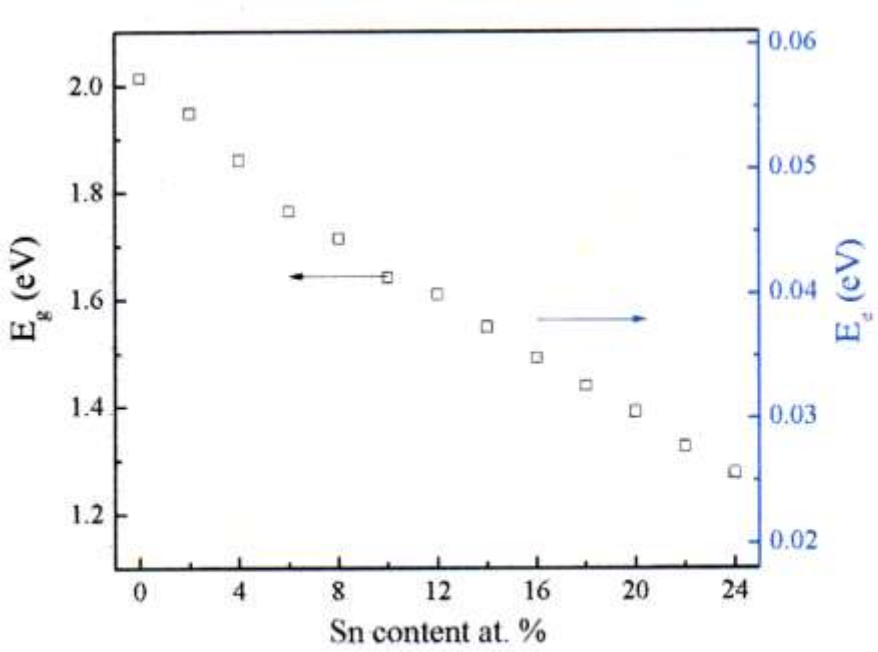

Fig. 4. Variations of E_g and E_c values with Sn content for $Sn_x(GeSe_2)_{100-x}$ ($0 \leq x \leq 24$ at. %) thin films.

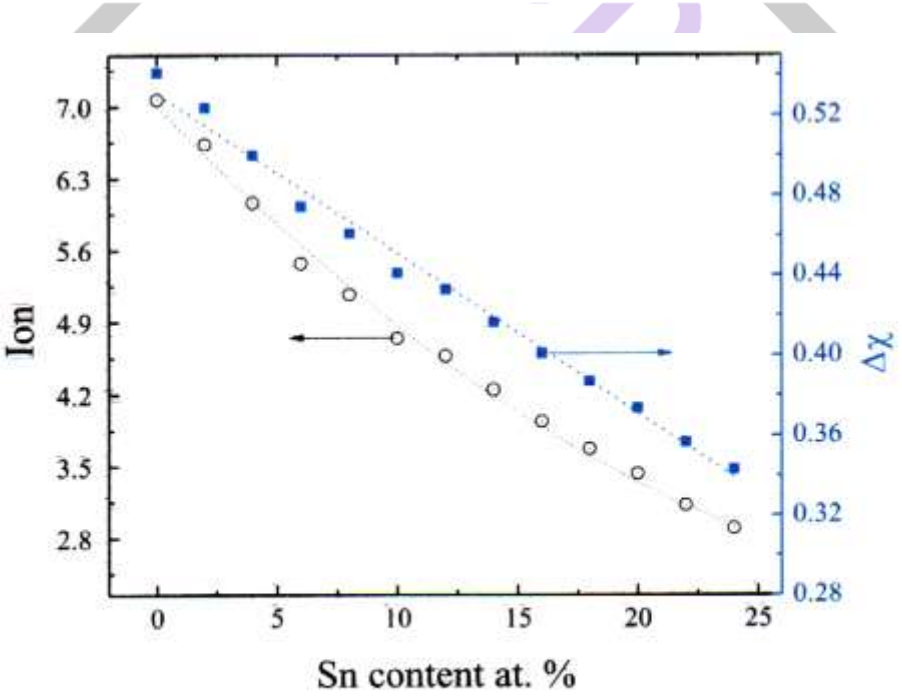

Fig. 5. Plots of $\Delta\chi$ and *Ion* versus Sn content for $Sn_x(GeSe_2)_{100-x}$ ($0 \leq x \leq 24$ at. %) thin films.

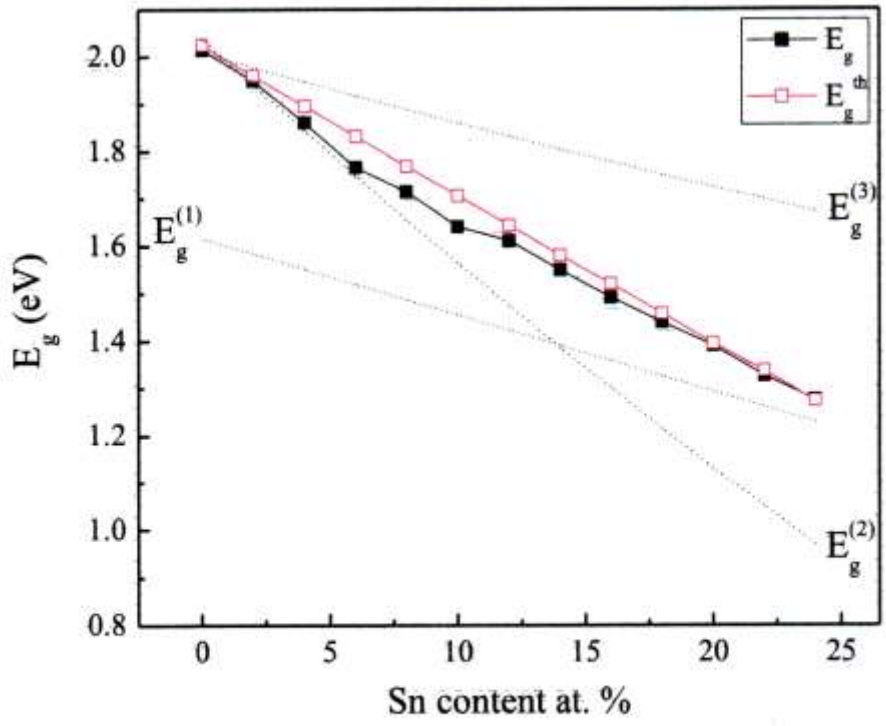

Fig. 6. Theoretical estimations (according to equations (11)-(13) and (15)) of the variations of the band gap with Sn content compared to experimental values (E_g) for $Sn_x(GeSe_2)_{100-x}$ ($0 \leq x \leq 24$ at. %) thin films.

$$E_g^{(2)} = D_{Sn-Se}.E_g(SnSe_2) + D_{Ge-Se}.E_g(GeSe_2) + D_{Ge-Ge}.E_g(Ge) \quad (12)$$

D_{Sn-Se}, D_{Ge-Se} and D_{Ge-Ge} are the portions of the corresponding bonds (see Table 3). This second method has the advantage of taking into account the local surrounding of each atom as predicted by chemical bond approach

Third, using Eq. (9), one could estimate the band gap from theoretical estimation of the overall $\Delta\chi$th, this third method can be qualified as mean field method since it uses the average overall electronegativity ignoring the local structure and bonding.

$$E_g^{(3)} = \Delta X_{th}/0.2688 \quad (13)$$

Where $\Delta\chi_{th}$ is the calculated overall electronegativity of the compound $Sn_x(GeSe_2)_{100-x}$ as following:

$$\Delta X_{th} = D_{Sn-Se}.|X_{Sn} - X_{Se}| + D_{Ge-Se}.|X_{Ge} - X_{se}| \quad (14)$$

One could notice in Fig. 6, that the $E_g^{(2)}$ underestimate the experimental band gap whereas $E_g^{(3)}$ overestimate it. Hence their average could be a good approximation as shown in the same figure:

$$E_g^{th} = \sqrt{E_g^{(2)}.E_g^{(3)}} \quad (15)$$

Clearly the last theoretical estimation of the band gap is in a good agreement with the optically measured ones. This could be explained by the fact that I combined two approximations an overall one ($E_g^{(3)}$) and a more local one ($E_g^{(2)}$).

The positions of the top energy level in the valence band (E_{VB}) as well as the minimum energy level in the conduction band (E_{CB}) are very important to be evaluated mainly for designing semiconductor devices. The E_{CB} and E_{VB} in eV can be theoretically estimated from the electron affinity (*EEA*), ionization energy (E_{Ion}) and the band gap energy (E_g) [41–44]. E_{CB} and E_{VB} for $Ge_\alpha Se_\beta Sn_\gamma$ have been estimated as the following:

$$E_{CB} = E_c - X + \frac{E_g}{2} \; and \; E_{VB} = E_C - X - \frac{E_g}{2} \quad (16)$$

Where

$$X = \left[(X_{Ge})^{\alpha}.(X_{Se})^{\beta}.(X_{Sn})^{\gamma}\right]^{1/(\alpha+\beta+\gamma)} \quad (17)$$

X_{Ge}, X_{Se} and X_{Sn} are the average values (E_{EA} + E_{Ion})/2 for Ge, Se and Sn, respectively. E_C is an energy constant, E_C = 4.5 eV [41,42], and X is a parameter of energy dimensions. Using elements' E_{EA} (1.235, 2.024, and 1.112 eV for Ge, Se, and Sn, respectively) and E_{ION} (7.910, 9.767, and 7.344 eV for Ge, Se, and Sn, respectively) [41,45], X_{Ge}, X_{Se}, X_{Sn} and hence X were obtained.

The estimated values of X, E_{CB} and E_{VB} listed in Table 3. As well, E_{VB} and E_{CB} are graphically depicted in Fig. 7. This figure shows that E_{VB} increases whereas ECB is almost constant with Sn content in $Sn_x(GeSe_2)_{100-x}$ system. Obviously, compounds with Sn content less than 6 at% have their band gap in the visible range. The rest of the prepared samples have an E_g in the infrared range. Since the maximum solar spectrum is around 1.48 eV one could expect that samples with compositions around 16 at% ($E_g \approx 1.49$ ev) will be suitable for solar cells.

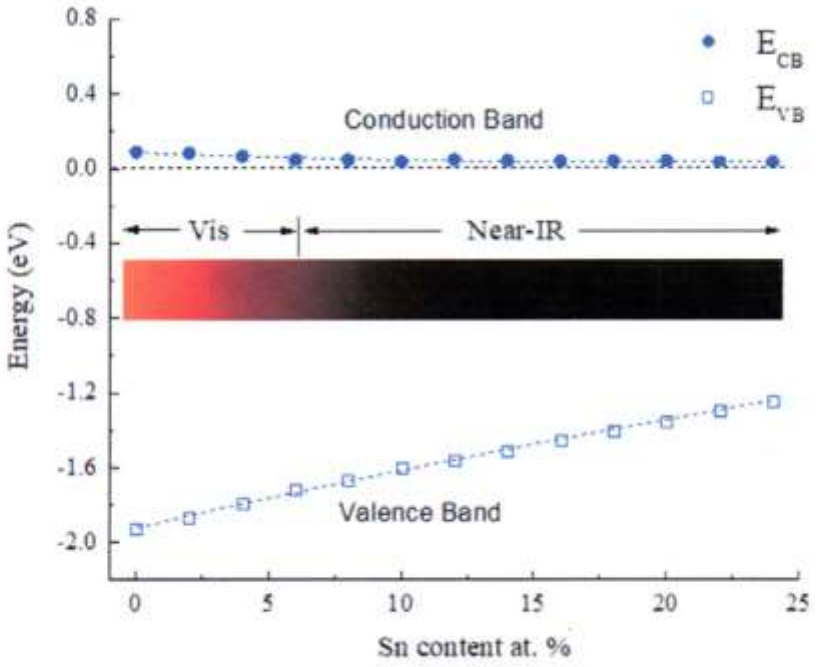

Fig. 7. The positions of the top energy level in the valence band (E_{VB}) as well as the minimum energy level in the conduction band (E_{CB}) versus Sn content for the $Sn_x(GeSe_2)_{100-x}$ ($0 \le x \le 24$ at. %) thin films.

4. Conclusions

Glasses of ternary Ge-Se-Sn with the composition $Sn_x(GeSe_2)_{100-x}$ ($0 \le x \le 24$ at. %) have been prepared as bulk and thin film samples. Sn atom is denser and more massive than Ge and/or Se atoms. Therefore, both the glass density and the mean atomic volume are increased while the glass compactness is decreased with the increment of Sn content. Introducing progressively Sn in the structure, induces the progressive replacement of Ge-Se bonds with Se-Sn and Ge-Ge bonds. The absorption coefficient (α) has been determined from the measured film absorbance (A). A clear red shift was observed with the addition of Sn amount, indicating a decrease of the band gap. Different theoretical estimations of the band gap variations with the composition were presented. One found a best adjustment to the experimental band gap when combining weighted contribution of the formed bonds.

The band gap tuning when changing composition from 2.01 to 1.28 eV, makes these glasses suitable for absorption in the major range of solar spectrum and therefore potential candidates for photo-voltaic applications.

Acknowledgement

The author extend his appreciation to the Dean Science J.P.U., Chapra, Prof. Udai Arvind, Prof. (Dr.) Rabindra Singh HOD, Deptt. Of Chemistry, J.P. University, Chapra, Rtd. Prof. & Former Head of Deptt. Of Chemistry, M.U., Bodh Gaya, Prof. (Dr.) R.P.S. Chauhan Saheb for their technical and administrative support.

References

1. J.S. Sanghera, L.B. Shaw, I.D. Aggarwal, Chalcogenide glass-fiber-based mid-IR sources and applications, IEEE J. Sel. Top. Quant. Electron. 15 (1) (2009) 114–119.
2. I.D. Aggarwal, J.S. Sanghera, Development and applications of chalcogenide glass optical fibers at NRL, J. Optoelectron. Adv. Mater. 4 (3) (2002) 665–678.
3. M. Eiichi, Amorphous built-in-field effect photoreceptors, Jpn. J. Appl. Phys. 21 (2) (1980) 213–223.

4. D.C. Hunt, S.S. Kirby, J.A. Rowlands, X-ray imaging with amorphous selenium: X-ray to charge conversion gain and avalanche multiplication gain, Med. Phys. 29 (11) (2002) 2464–2471.
5. K.A. Aly, A. Dahshan, A.M. Abousehly, Compositional dependence of the optical properties of amorphous Se100-xTex thin films, Philos. Mag. A 88 (1) (2008) 47–60.
6. S.S. Fouad, S.A. Faek, S.M. El-Sayed, Spectroscopic studies in glassy semiconducting GexSe1-x, Vacuum 53 (3) (1999) 415–419.
7. A.K. Dixit, P. Sharma, A. Thakur, V. Mishra, P. Sharma, V.S. Rangra, Compositional dependence of physical parameters in Sn-Se in chalcogenide glasses, Chalcogenide Lett. 12 (5) (2015) 249–256.
8. D. Tonchev, B. Fogal, G. Belev, R.E. Johanson, S.O. Kasap, Properties of a-SbxSe1-x photoconductors, J. Non-Cryst. Solids 299–302 (2002) 998–1001.
9. P. Sharma, A. Dahshan, V.K. Sehgal, K.A. Aly, High thermoelectric action in vacuum deposited indium alloyed chalcogenide thin films: InxSe100-x, IEEE Trans. Electron. Dev. 65 (8) (2018) 3408–3413.
10. V. Kumari, A. Kaswan, D. Patidar, N. Saxena, K. Sharma, I-V measurements of Ge- Se-Sn chalcogenide glassy alloys, Process. Applic. Ceramics 9 (1) (2015) 61–66.
11. F. Serrano-Sanchez, N.M. Nemes, J.L. Martínez, O. Juan-Dura, M.A. de la Torre, M. T. Fernandez-Díaz, J.A. Alonso, Structural evolution of a Ge-substituted SnSe thermoelectric material with low thermal conductivity, J. Appl. Crystallogr. 51 (2) (2018) 337–343.
12. H. Singh Deepika, N.S. Saxena, Optical characterization of nanostructured Ge1 □ xSnxSe2.5 (x ¼ 0, 0.3, 0.5) films, Opt. Quant. Electron. 51 (11) (2018) 1–11.
13. A. Thakur, V. Sharma, P.S. Chandel, N. Goyal, G.S.S. Saini, S.K. Tripathi, Photoconductivity in thin film of a-(Ge20Se80)0.90Sn0.10, J. Mater. Sci. 41 (8) (2006) 2327–2332.
14. S.A. Fayek, The effects of Sn addition on properties and structure in Ge–Se chalcogenide glass, Infra, Phys. Technol. 46 (3) (2005) 193–198.
15. A.Z. Mahmoud, M. Mohamed, S. Moustafa, A.M. Abdelraheem, M.A. Abdel-Rahim, Study of non-isothermal crystallization kinetics of $Ge_{20}Se_{70}Sn_{10}$ chalcogenide glass, J. Therm. Anal. Calorim. 131 (3) (2017) 2433–2442.
16. M.I. Abd-Elrahman, M.M. Hafiz, A.M. Abdelraheem, A.A. Abu-Sehly, Effect of Sn additive on the structure and crystallization kinetics in Ge–Se alloy, J. All. Comp. 675 (2016) 1–7.
17. H.-y. Chen, S.-w. Chen, S.-h. Wu, Glass formation, physical properties and optical properties of Ge–Se–Sn and Ge–Sb–Se–Sn alloys, Mater. Chem. Phys. 80 (2003)
18. A.A.A. Darwish, M. Rashad, A.E. Bekheet, M.M. El-Nahass, Linear and nonlinear optical properties of $GeSe_{2-x}Sn_x$ ($0 \leq x \leq 0.8$) thin films for optoelectronic applications, J. All. Comp. 709 (2017) 640–645.
19. H.M. Kotb, F.M. Abdel-Rahim, The influence of the substitution of Se for Sn on the thermal, optical and dispersion properties of $Ge_{14}Se_{86-x}Sn_x$ thin films, Mater. Sci. Semicond. Process. 38 (2015) 209–217.
20. K.A. Aly, On the study of the optical constants for different compositions of Sn x $(GeSe)_{100-x}$ thin films in terms of the electronic polarizability, electronegativity and bulk modulus, Appl. Phys. A 120 (1) (2015) 293–299.
21. P. Bavafa, M. Rezvani, Effect of Sn doping in optical properties of Se-Ge glass and glass-ceramics, Results in Physics 10 (2018) 777–783.
22. J. Bicerano, S.R. Ovshinsky, Chemical bond approach to the structures of chalcogenide glasses with reversible switching properties, J. Non-Cryst. Solids 74 (1985) 75–84.
23. J. Bicerano, S.R. Ovshinsky, Chemical bond approach to glass structure, J. Non- Cryst. Solids 75 (1985) 169–175.
24. A. Dahshan, K.A. Aly, Characterization of new quaternary Ge20Se60Sb20□ xAgx ($0 \leq x \leq 20$ at.%) glasses, J. Non-Cryst. Solids 408 (2015) 62–65.
25. A. Ioffe, A. Regel, Non-crystalline, amorphous and liquid electronic semiconductors, Prog. Semicond. 4 (1960) 237–291.
26. J.C. Phillips, M.F. Thorpe, Constraint theory, vector percolation and glass formation, Solid State Commun. 53 (1985) 699–702.
27. A. Dahshan, H.H. Hegazy, K.A. Aly, Effect of Sn addition on physical and optical properties of Ge-Se-Sb-Sn thin films, Chalcogenide Lett. 15 (2018) 545–553.
28. L. Zhenhua, Chemical bond approach to the chalcogenide glass forming tendency, J. Non-Cryst. Solids 127 (1991) 298–305.
29. A. Dahshan, New amorphous As–Se–Sb–Cu thin films: theoretical characterization and evaluation of optical constants, Appl. Phys. A 123 (210) (2017) 1–6.
30. L. Tichy, A. Triska, H. Ticha, M. Frumar, J. Klikorka, The composition dependence of the gap in amorphous films of $SixGe_{1-x}$, $SbxSe_{1-x}$ and $AsxTe_{1-x}$ systems, Solid State Commun. 41 (1982) 751–754.
31. L. Pauling, The Nature of the Chemical Bond, Cornell university press, New York, 1960.
32. H.H. Hegazy, A. Dahshan, K.A. Aly, Influence of Cu content on physical characterization and optical properties of new amorphous Ge–Se–Sb–Cu thin films, Mater. Res. Express 6 (2) (2019) 1–8.
33. S.R. Alharbi, K.A. Aly, E.S. Al-zahrani, A. Dahshan, W. Alharbi, Physical behavior of As-Se-Se glasses with constant coordination number (NC = 2.2), Chalcogenide Lett. 15 (2018) 339–343.
34. E.S¸. Tüzemen, S. Eker, H. Kavak, R. Esen, Dependence of film thickness on the structural and optical properties of ZnO thin films, Appl. Surf. Sci. 255 (2009) 6195–6200.
35. K.A. Aly, Optical constants of quaternary Ge-As-Te-In amorphous thin films evaluated from their reflectance spectra, Philos. Mag. A 89 (12) (2009) 1063–1079.

36. K.A. Aly, Optical band gap and refractive index dispersion parameters of $As_xSe_{70}Te_{30-x}$ ($0 \leq x \leq 30$ at.%) amorphous films, Appl. Phys. Mater. Sci. Process 99 (4) (2010) 913–919.
37. N.F. Mott, E.A. Davis, Electronic Processes in Non-crystalline Materials, Oxford University Press, London, 1971.
38. J.A. Duffy, Trends in energy gaps of binary compounds : an approach based upon electron transfer parameters from optical spectroscopy, J. Phys. C Solid State Phys. 13 (1980) 2979–2989.
39. P. Moontragoon, Z. Ikonic, P. Harrison, Band structure calculations of Si–Ge–Sn alloys: achieving direct band gap materials, Semicond. Sci. Technol. 22 (2007) 742–748.
40. L. Tichy, A. Triska, H. Ticha, M. Frumar, J. Klikorka, The composition dependence of the gap in amorphous films of Si_xGe_{l-x}, Sb_xSe_{l-x} and As_xTe_{1-x} systems, Solid State Commun. 41 (10) (1982) 751–754.
41. A.S. Hassanien, I. Sharma, Band-gap engineering, conduction and valence band positions of thermally evaporated amorphous Ge_{15-x} Sb_x Se_{50} Te_{35} thin films: influences of Sb upon some optical characterizations and physical parameters, J. All. Comp. 798 (2019) 750–763.
42. M. Askari, N. Soltani, E. Saion, W.M.M. Yunus, H. Maryam Erfani, M. Dorostkar, Structural and optical properties of PVP-capped nanocrystalline $Zn_xCd_{1-x}S$ solid solutions, Superlattice. Microst. 81 (2015) 193–201.
43. R. Xie, J. Su, Y. Liu, L. Guo, Optical, structural and photoelectrochemical properties of $CdS_{1-x}Se_x$ semiconductor films produced by chemical bath deposition, Int. J. Hydrogen Energy 39 (7) (2014) 3517–3527.
44. C. Xing, Y. Zhang, W. Yan, L. Guo, Band structure-controlled solid solution of $Cd_{1-x}Zn_xS$ photocatalyst for hydrogen production by water splitting, Int. J. Hydrogen Energy 31 (14) (2006) 2018–2024.
45. S.G. Bratsch, J. Lagowski, Predicted stabilities of monatomic anions in water and liquid ammonia at 298.15 K, Polyhedron 5 (11) (1986) 1763–1770.